J Mater Sci (2009) 44:4604–4612
DOI 10.1007/s10853-009-3702-6

Finite element simulation of complex interfacial segregation phenomena in dilute alloys

F. Tancret · F. Fournier Dit Chabert · F. Christien · R. Le Gall

Received: 21 November 2008 / Accepted: 20 June 2009 / Published online: 11 July 2009

Abstract Segregation of trace elements on a surface, at grain boundaries or more generally in any interface can have important consequences: adhesion of thin films, catalytic activity, embrittlement of steels by P or of nickel alloys by S, reinforcement of nickel alloys by B, etc. Segregation kinetics can be simulated by a finite element (FE) approach, by implementing the Darken–Du Plessis equation at the interface and Fick's diffusion laws in the bulk. It is then possible to simulate segregation kinetics in non-isothermal conditions, and to couple segregation and macroscopic heat transfer calculations. A previously developed model is here adapted to the case of complex interfacial segregation phenomena: (i) segregation of a single species with a solute–solute or solute–solvent interaction, (ii) co-segregation of two species with a site competition in the interface, and (iii) segregation of a single species at an interface between two phases. Results are compared with available experimental data.

Introduction and background

The classical theory of interfacial segregation: thermodynamics and kinetics

Given their singular atomic structures, interfaces in materials possess peculiar chemical, physical and mechanical properties. Interfaces can be of different kinds: free surfaces, grain boundaries, interdendritic boundaries, interphase boundaries, etc. Among others, chemical equilibria in interfaces are modified compared to the bulk, with different thermodynamic conditions for the formation of solid solutions and/or ordered phases. In nickel for example, despite an extremely low bulk solubility of sulfur, the surface and/or grain boundary atomic concentrations can reach several tens of percent in certain conditions [1]. This phenomenon is known as interfacial segregation [2]. It can, in some cases, induce important modifications of the properties of materials, in particular an intergranular embrittlement of metals and alloys (nickel, iron, steels, etc.) by impurities such as sulfur and/or phosphorus [3]. The equilibrium between the interface and the bulk can be expressed by the following thermodynamic equation [4, 5]:

$$\frac{X^{\varphi}_{\mathrm{I,eq}}}{X^{\varphi}_{\mathrm{I,max}} - X^{\varphi}_{\mathrm{I,eq}}} = \frac{X^{\mathrm{v}}_{\mathrm{I}}}{1 - X^{\mathrm{v}}_{\mathrm{I}}} \exp\left(-\frac{\Delta G_{\mathrm{I}}}{RT}\right) \quad (1)$$

where ΔG_{I} is the free energy for segregation of the solute I, $X^{\varphi}_{\mathrm{I,eq}}$ the equilibrium interfacial atomic fraction of solute, $X^{\varphi}_{\mathrm{I,max}}$ the maximum fraction of sites in the interface that can be occupied by the solute atoms (it is equal to unity if the segregation is perfectly substitutional and lower if for geometrical reasons, all the sites cannot be occupied by the solute), $X^{\mathrm{v}}_{\mathrm{I}}$ the bulk atomic fraction of free solute ("free" meaning that, for instance, solutes trapped in precipitates or yet segregated are not taken into account), R the gas constant, and T the temperature. A common practice is to introduce a new quantity, called the equilibrium coverage ratio of the interface, $\theta_{\mathrm{I,eq}}$, defined as the ratio between the equilibrium fraction of solute in the interface and the maximum value, $\frac{X^{\varphi}_{\mathrm{I,eq}}}{X^{\varphi}_{\mathrm{I,max}}}$. Then, replacing $\frac{X^{\varphi}_{\mathrm{I,eq}}}{X^{\varphi}_{\mathrm{I,max}}}$ by $\theta_{\mathrm{I,eq}}$ Eq. 1 becomes:

F. Tancret (✉) · F. Fournier Dit Chabert · F. Christien · R. Le Gall
Université de Nantes, Nantes Atlantique Universités, Polytech'Nantes, LGMPA, Rue Christian Pauc, BP 50609, 44306 Nantes Cedex 3, France
e-mail: franck.tancret@univ-nantes.fr

$$\frac{\theta_{\mathrm{I,eq}}}{1-\theta_{\mathrm{I,eq}}} = \frac{X_{\mathrm{I}}^{\mathrm{v}}}{1-X_{\mathrm{I}}^{\mathrm{v}}} \exp\left(-\frac{\Delta G_{\mathrm{I}}}{RT}\right) \quad (2)$$

This thermodynamic approach dictates that the coverage ratio decreases as temperature increases, as shown on the example of Fig. 1. Nevertheless, since in reality, the interfacial and bulk concentrations can be very different (several orders of magnitude), in order to reach this equilibrium, there must be a diffusional transport of the segregation species between the bulk and the interface. The equilibrium coverage ratio can therefore be reached in "reasonable" times only for quite high temperatures, where diffusion is fast enough; segregation kinetics is at the opposite strongly limited by diffusion at low temperatures. For instance, in the case of a material in which segregation has been previously removed by a high temperature heat treatment, three different situations can be usually found: (i) temperature is high enough so that the equilibrium coverage ratio remains low; (ii) temperature is low and diffusion is so slow that segregation cannot occur for kinetic reasons, even if the equilibrium coverage ratio is high; (iii) in an "intermediate" range of temperatures, diffusion is fast enough so that significant coverage ratios can be reached within times that are characteristic of real situations (service conditions or processing). This is, for example, responsible for a loss of ductility in nickel-based alloys in the temperature range ~700–1000 °C, due to the segregation of sulfur at grain boundaries [3].

In the past, analytic equations have been successfully derived to predict the evolution of segregation with time and temperature, but in most "real" cases, these equations cannot be used, especially when temperature depends on time and is not uniform in the specimen. Therefore, several numerical approaches have also been proposed to deal with such cases. In particular, finite element (FE) models can, in addition to the calculation of segregation kinetics, predict with a good accuracy the thermal and stress fields in a specimen subjected to complex histories (for example welding, quenching, forging, etc). This is useful for engineering purposes, to calculate the segregation level at any time and any position of a real part and eventually to predict the probability of failure, in the case of segregation of tramp elements. Preliminary study on these aspects is summarized in the next section.

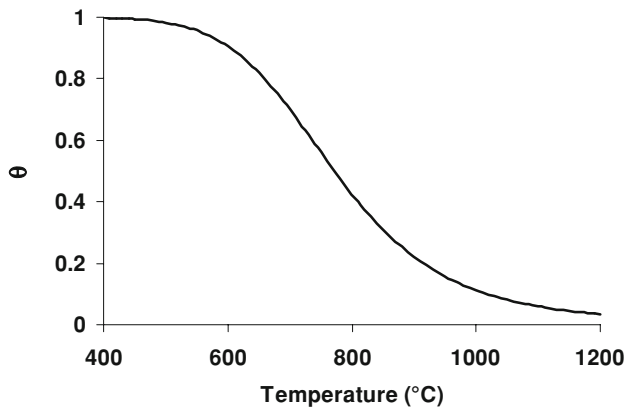

Fig. 1 Evolution with temperature of the equilibrium coverage ratio, calculated with $X_{\mathrm{I}}^{\mathrm{V}} = 10$ at. ppm and $\Delta G_{\mathrm{I}} = -100$ kJ/mol

Finite element simulation of interfacial segregation: background

In a previous article [6], it has been shown that the kinetics of segregation could be simulated by a FE approach, by coupling the resolution of Fick's diffusion equations in the bulk to the Darken–Du Plessis model [7, 8] to govern the flux of exchange of solute between the interface and its vicinity in the bulk, J_{I}:

$$J_{\mathrm{I}} = -\frac{D_{\mathrm{I}} C_{\mathrm{I}}^{\mathrm{v}}(\varphi)}{\delta}\left(\frac{\Delta G_{\mathrm{I}}}{RT} + \ln\frac{\theta_{\mathrm{I}}\left(1-X_{\mathrm{I}}^{\mathrm{v}}(\varphi)\right)}{X_{\mathrm{I}}^{\mathrm{v}}(\varphi)(1-\theta_{\mathrm{I}})}\right) \quad (3)$$

where D_{I} is the bulk diffusion coefficient of the solute, δ the interatomic plane spacing, and θ_{I} the current (i.e., non-equilibrium) coverage ratio. $X_{\mathrm{I}}^{\mathrm{v}}(\varphi)$ and $C_{\mathrm{I}}^{\mathrm{v}}(\varphi)$ are, respectively, the atomic fraction and the concentration of the solute in the bulk at the vicinity of the interface. It can be seen that, when thermodynamic equilibrium is reached (i.e., Eqs. 1, 2 are fulfilled), the flux defined by Eq. 3 is equal to zero. In parallel, the evolution of the interfacial solute concentration, C_{I}^{φ}, is computed using:

$$\frac{\mathrm{d}C_{\mathrm{I}}^{\varphi}}{\mathrm{d}t} = -f \cdot J_{\mathrm{I}} \quad (4)$$

where f is a geometric coefficient. It is equal to unity for a surface and to two for a grain boundary, to take into account the gathering in the interface of solute coming from both adjacent grains. Both in the bulk and in the interface, the atomic fractions and concentrations ($X_{\mathrm{I}}^{\mathrm{v}}$ and $C_{\mathrm{I}}^{\mathrm{v}}$ on the one hand, X_{I}^{φ} and C_{I}^{φ} on the other hand) are related to each other through bulk and interface site densities (for example, in nickel, with a lattice parameter of 0.352 nm and a face centered cubic structure, the bulk site density is 9.17×10^{28} m^{-3} and the surface site density is 1.61×10^{19} m^{-2} on a (100) surface).

Equations 3 and 4 were implemented in the Comsol FE software and solved at the interface. They were coupled to a bulk diffusion model, where the diffusion coefficient was defined as $D_{\mathrm{I}} = D_{0\mathrm{I}} \exp\left(-Q_{\mathrm{I}}/RT\right)$, where $D_{0\mathrm{I}}$ and Q_{I} are the material-dependent properties [6]. All the features of interfacial segregation mentioned in "The classical theory of interfacial segregation: thermodynamics and kinetics" were well predicted by the model [6], including the competition between thermodynamics and kinetics in an intermediate range of temperatures. The model could be

used to simulate both surface segregation and grain boundary segregation, in non-isothermal conditions.

Complex cases

Nevertheless, in real cases, more complex interfacial phenomena can occur. In particular, it is well known that solute–solute or solute–matrix interactions can occur and modify the thermodynamics of segregation. Also, there are cases where several different solute species compete for the same segregation sites; this is the case, for example, of phosphorus and sulphur in iron, nickel, or iron–nickel based alloys. Finally, the segregation of a species at an interphase between two crystals of different nature is very important, for instance, in the case of polyphased alloys, coatings, cermets, etc. The aim of this article is to present an extension of the previously developed FE model [6] to such complex cases. Results will be assessed both on theoretical bases and through comparisons with published data, when available. As a general rule, no information will be given on the specific basic definition of the FE model (except when necessary and/or specific to the cases treated here), since these aspects have already been dealt with in a previous study [6].

Solute–solute or solute–solvent interaction

Physical phenomenon and basic equations

Even if it can often be neglected, the interfacial free energy for segregation of a given species, ΔG_I, is not a fixed value, but depends on the concentration of solute already segregated in the interface [4]. This can be expressed as:

$$\Delta G_I = \Delta G_I^0 - 2\alpha_{IM}(X_I^{\varphi} - X_I^{v}) \quad (5)$$

where α_{IM} can be seen as either a repulsive interaction between the solvent (matrix) atoms and the solute, or as an attractive solute–solute interaction in the interface, which would both produce the same effects: the segregation of a given solute "favors" the segregation of the same solute atoms (either by decreasing the repulsive effect of the solvent atoms or by increasing the attractive effect of the solute atoms), thereby increasing the driving force for segregation. Given the fact that the bulk concentration in dilute alloys is usually several orders of magnitude lower than the interfacial concentration, Eq. 5 reduces to:

$$\Delta G_I = \Delta G_I^0 - 2\alpha_{IM}X_I^{\varphi} \quad (6)$$

Such effects have been observed, for example, by Cornen [1] in high-purity nickel containing 7.2 at. ppm of sulfur: after a high-temperature heat treatment aiming at removing segregation, different agings were performed at temperatures ranging between 650 and 1100 °C, either after heating from 500 °C or after cooling down from 1100 °C, with durations long enough to reach equilibrium. Grain boundary segregation was then measured by an intergranular etching technique [1]. A strong hysteresis was obtained between heating and cooling conditions, as shown on Fig. 2: for instance, at 850 °C, coverage ratios of 0.90 and 0.02 were obtained after heating and cooling, respectively.

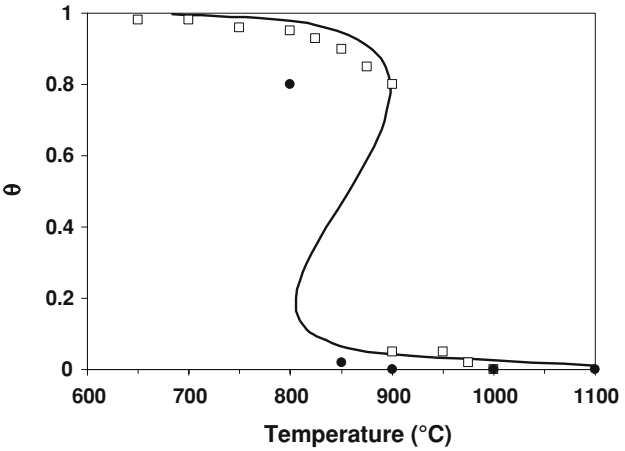

Fig. 2 Symbols: data from [1] (*squares*: after heating; *circles*: after cooling); *solid line*: Eq. 2 calculated using Eq. 6

This behavior can be explained by the "S"-shape taken by the equilibrium segregation curve in the case of an interaction, such as expressed in Eq. 6. A good description of the data gained by Cornen is shown on the curve of Fig. 2, drawn with $\Delta G_I^0 = -82$ kJ/mol and $2\alpha_{IM} = 117$ kJ/mol and with, in the case of sulfur in nickel, $\theta_I = 2X_I^{\varphi}$ [9]. For example, on heating from low temperatures up to 850 °C, sulfur first segregates strongly, due to a high equilibrium coverage ratio, and then θ_I follows the upper branch of the curve, leading to a high coverage ratio at 850 °C. At the opposite, on cooling from high temperatures down to 850 °C, the coverage ratio follows the lower branch of the curve, leading to a low coverage ratio at 850 °C. Thus, depending on the thermal history, two different equilibria can be reached for the same temperature.

Finite element simulation and results

The modification expressed in Eq. 6, i.e., the dependence of ΔG_I on X_I^{φ} has been brought to the already existing FE model: a scalar expression for the free energy of segregation has been created in Comsol, as in Eq. 6, which is then used in Eq. 3 instead of a fixed value for ΔG_I. The numerical resolution of such a system of equations needs, however, a certain control of the time steps taken by the

solver, since quite steep variations in the solution can occur due to the creation of a "circular reference" (the evolution with time of X_I^{φ} depends on ΔG_I, which itself depends on X_I^{φ}): in Comsol, time steps taken by the UMFPACK solver must be set as "Strict" or "Intermediate," and not "Free". The diffusion coefficient is also entered as a scalar variable, with $D_{0I} = 1.4 \times 10^{-4}$ m^2/s and $Q_I = 219$ kJ/mol (as in [1]), to take temperature into account.

Among others, isothermal agings were simulated at various temperatures, either starting from a non-segregated state (corresponding to a previous high temperature heat treatment) or from a highly segregated state (corresponding to a previous low temperature heat treatment). Results are in good agreement with the above-mentioned features, given the fact that the two extrema of the "S"-shape curve of Fig. 2 are at 804.9 and 898.2 °C:

- When simulating segregation heat treatments at 804 °C or below (starting from a non-segregated state), the coverage ratio tends toward a high value (Fig. 3a), with a first metastable plateau when temperature is close to the extremum of the "S"-curve (e.g., at 804 °C).
- When simulating segregation heat treatments at 805 °C or above (starting from a non-segregated state), the coverage ratio tends toward a low value (Fig. 3a).
- When simulating desegregation heat treatments at 899 °C or above (starting from a highly segregated state), the coverage ratio tends toward a low value (Fig. 3b), with a first metastable plateau when temperature is close to the extremum of the "S"-curve (e.g., at 899 °C).
- When simulating desegregation heat treatments at 898 °C or below (starting from a highly segregated state), the coverage ratio tends toward a high value (Fig. 3b).

The model therefore allows to simulate segregation kinetics in the case of strong solute–solute or solute–solvent interactions.

Segregation site competition

Physical phenomenon and basic equations

In real alloys, several different species can segregate simultaneously; this phenomenon is called co-segregation. In the case where all species occupy the same kind of segregation sites (e.g., substitutional), they have to compete to segregate at interfaces, since the total number of segregation sites is limited. This is the case, for instance, of sulfur and phosphorus in iron, nickel and iron–nickel alloys. The equations describing such a system are rather simple and derive from Eqs. 1 to 3. The latter just need to be modified to take into account the fact that the total interfacial concentration is the sum of concentrations for all solutes. For example, for two solutes I and J, Eq. 1 simply becomes [4, 10]:

$$\frac{X_{i,eq}^{\varphi}}{X_{max}^{\varphi} - X_{I,eq}^{\varphi} - X_{J,eq}^{\varphi}} = \frac{X_i^{v}}{1 - X_I^{v} - X_J^{v}} \exp\left(-\frac{\Delta G_i}{RT}\right) \tag{7}$$

where i can be either I or J. In this equation X_{max}^{φ} is the maximum total interfacial atomic fraction of segregants (maximum possible value for the sum $X_I^{\varphi} + X_J^{\varphi}$). As in the situations exposed in previous sections, this equilibrium condition corresponds to a state where the fluxes at the interface (as in Eq. 3) are equal to zero. Using the coverage ratios for segregating species, $\theta_i = \frac{X_i^{\varphi}}{X_{max}^{\varphi}}$, the fluxes are here expressed as:

$$J_i = -\frac{D_i C_i^{v}(\varphi)}{\delta}\left(\frac{\Delta G_i}{RT} + \ln\frac{\theta_i\left(1 - X_I^{v}(\varphi) - X_J^{v}(\varphi)\right)}{X_i^{v}(\varphi)(1 - \theta_I - \theta_J)}\right) \tag{8}$$

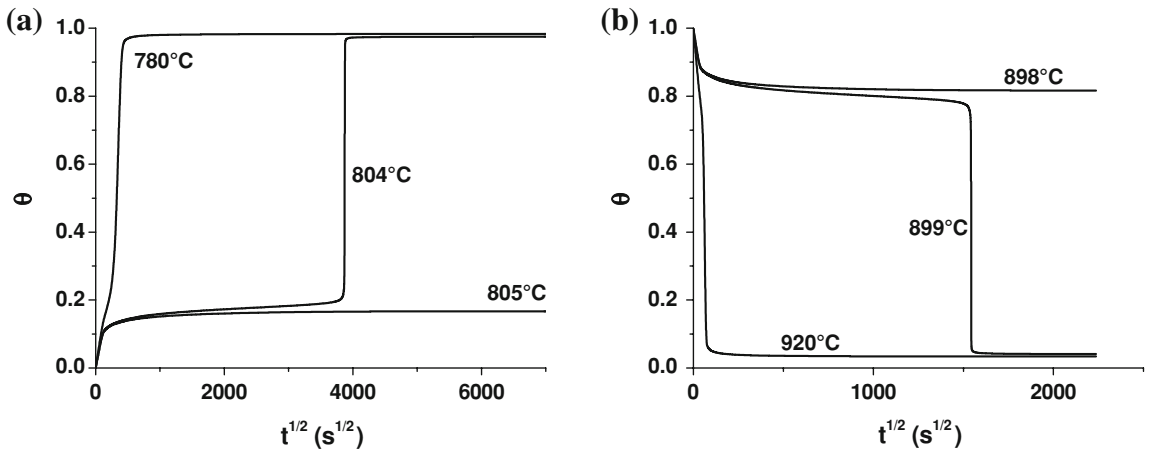

Fig. 3 Calculated isothermal kinetics of **a** segregation and **b** desegregation

In parallel, two equations such as Eq. 4 (one for I and one for J), and two bulk diffusion models must also be solved simultaneously, one for each segregating species.

Finite element simulation and results

In practice, in the software, there is a need to define two diffusion modes in the bulk and two "weak" modes in the interface to govern the evolutions of interfacial concentrations with time (one of each for each segregating species). For the two diffusion modes, defined in a single geometry, the boundary conditions are the fluxes, expressed as in Eq. 8 and entered separately as "boundary expressions". For the two interfacial "weak" modes, the boundary conditions are expressed as in Eq. 4 (one for each segregating species).

Results are shown in Fig. 4 for an illustrative example, in the case of the isothermal surface segregation kinetics of two species (I and J) at 600 °C, starting from a non-segregated state, and calculated with the following values: $X_I^v = X_J^v = 20$ at. ppm, $Q_I = Q_J = 200$ kJ/mol, $D_{0I} = 2 \times 10^{-3}$ m^2/s, $D_{0J} = 2 \times 10^{-5}$ m^2/s, $\Delta G_I = -90$ kJ/mol, $\Delta G_J = -120$ kJ/mol.

As expected from theory, impurity I first segregates more rapidly than impurity J, since its mobility is two orders of magnitude higher. However, impurity J is more stable in the interface than impurity I (due to different ΔG_i values), and will thus, after a while, segregate preferentially at the interface by replacing progressively impurity I, the latter being eventually forced to desegregate when the total coverage ratio approaches one.

Case study: phosphorus and sulfur in a Fe–Ni alloy

In iron, nickel, or iron–nickel alloys, substitutional solutes like sulfur and phosphorus compete for the same interfacial segregation sites. In particular, the phenomenon described in "Finite element simulation and results" have been observed by Ben Mostefa Daho [11, 12] in an Invar alloy (Fe–36 wt.% Ni) containing $X_P^v = 55$ at. ppm and $X_S^v = 32$ at. ppm. During an isothermal aging at 700 °C, the evolutions of phosphorus and sulfur superficial segregations were measured in situ by Auger Electron Spectroscopy (AES). After conversion of the published raw AES measurements into coverage ratios (see Appendix 1), the data presented in Fig. 5 are obtained. At 700 °C, the mobility of P is higher than that of S, and phosphorus first segregates faster than sulfur. But sulfur is more stable on the surface than phosphorus, and it continues to segregate and progressively forces phosphorus to desegregate.

However, two aspects of the measured kinetics cannot be correctly explained by a site competition only. Indeed, on the one hand, phosphorus desegregation starts to occur for a total coverage ratio ($\theta_P + \theta_S$) that is somewhat lower than unity ($\sim$0.8), and on the other hand, phosphorus desegregation is very fast, whereas the desegregation provoked by a sole site competition is generally a smooth process, as illustrated on Fig. 4. These features can only be explained (and simulated) if a repulsive interaction exists [13] between phosphorus and sulfur: when S starts to segregate, not only it competes with P for segregation sites, but it also decreases its driving force for segregation. Phosphorus becomes therefore less and less stable in the interface as sulfur segregation proceeds. This can be expressed in the model by introducing a phosphorus–sulfur interaction term, α_{PS}, in the segregation free energies, as [4, 10]:

$$\Delta G_P = \Delta G_P^0 - 2\alpha_{PS} X_S^{\varphi} \text{ and } \Delta G_S = \Delta G_S^0 - 2\alpha_{PS} X_P^{\varphi} \qquad (9)$$

A reasonable fit of the measurements can be obtained with $D_P = 9 \times 10^{-15}$ m^2/s, $D_S = 9 \times 10^{-17}$ m^2/s, $\Delta G_P^0 =$

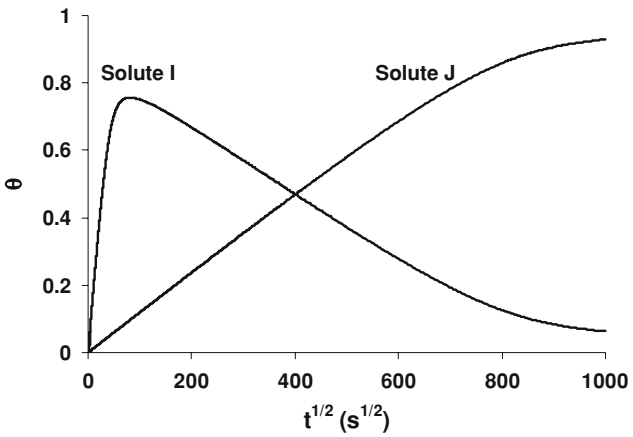

Fig. 4 Example of cosegregation kinetics with a site competition

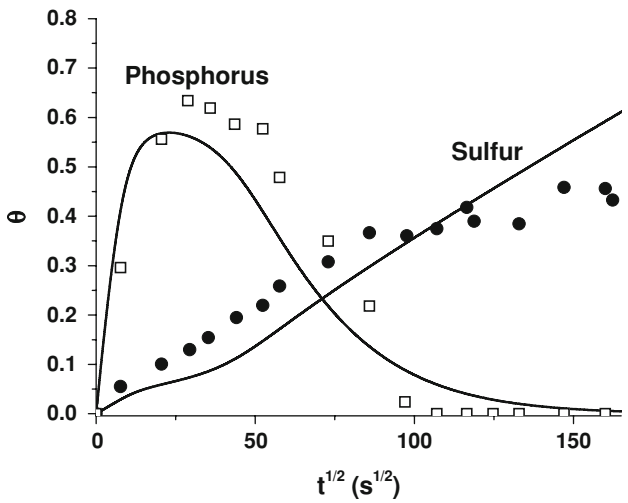

Fig. 5 Comparison between calculated (*solid lines*) and measured (symbols, data from [11, 12]) cosegregation kinetics of P and S on the surface of an Invar alloy at 700 °C

-90 kJ/mol, $\Delta G_S^0 = -120$ kJ/mol and $2\alpha_{PS} = -150$ kJ/mol, as shown on Fig. 5.

It should be noted that, as in "Solute–solute or solute–solvent interaction", it would have been possible to introduce also a sulfur–sulfur interaction. Qualitatively, this would have meant that the driving force for sulfur segregation increases as sulfur progressively arrives on the surface, hence forcing phosphorus to leave faster. This possibility has been tested but

- Taken alone (i.e., instead of the P–S interaction), it was not possible to simulate experimental data in a satisfactory manner.
- Taken in addition to the P–S interaction, on the one hand, it did not seem to bring any significant improvement over the sole P–S interaction, and on the other hand, it became extremely difficult to adjust all the parameters simultaneously to the data.

Interphase segregation

Physical phenomenon and basic equations

In some systems, for instance in polyphased alloys, in thin films, or in composites like cermets, interfaces exist between different phases, i.e., between crystals of a different nature. Solute segregation can occur at these interfaces (called interphases), which is known as interphase segregation. In order to deal with such cases, it is first necessary to consider the equilibrium state of the system: the solute must be simultaneously in equilibrium with both phases and the interphase. Rewriting Eq. 1 gives:

$$\frac{X^{\varphi}_{I,eq}}{X^{\varphi}_{I,max} - X^{\varphi}_{I,eq}} = \frac{X^{v}_{I1}}{1 - X^{v}_{I1}} \exp\left(-\frac{\Delta G_{I1}}{RT}\right) = \frac{X^{v}_{I2}}{1 - X^{v}_{I2}} \exp\left(-\frac{\Delta G_{I2}}{RT}\right) \quad (10)$$

where the subscripts 1 and 2 refer to the two phases. This condition implies that each bulk phase is also in equilibrium with the other one (if phase 1 is in equilibrium with the interface, and the latter in equilibrium with phase 2, then phases 1 and 2 are also in equilibrium with each other). Then, using Eq. 10, stating that the total solute quantity must remain constant, and considering that the quantity of solute in the interphase is negligible compared to those in the bulk phases (which is often true), one gets

$$\frac{X^{\varphi}_{I,eq}}{X^{\varphi}_{I,max} - X^{\varphi}_{I,eq}} = \frac{\theta_I}{1 - \theta_I} = \frac{N_1 X^{v}_{I1} + N_2 X^{v}_{I2}}{N_1 \exp\left(\frac{\Delta G_{I1}}{RT}\right) + N_2 \exp\left(\frac{\Delta G_{I2}}{RT}\right)} \quad (11)$$

where N_1 and N_2 are the numbers of solvent atoms in bulk phases 1 and 2. In what follows, for simplicity reasons, only the particular case where $N_1 = N_2$ will be considered, although the general case can also be addressed. Eq. 11 reduces to

$$\frac{X^{\varphi}_{I,eq}}{X^{\varphi}_{I,max} - X^{\varphi}_{I,eq}} = \frac{\theta_I}{1 - \theta_I} = \frac{X^{v}_{I1} + X^{v}_{I2}}{\exp\left(\frac{\Delta G_{I1}}{RT}\right) + \exp\left(\frac{\Delta G_{I2}}{RT}\right)} \quad (12)$$

Looking at this equation, and given the fact that Eq. 10 must be fulfilled simultaneously, it appears that the equilibrium at a certain temperature is possible with only one set of values for the concentrations of solute in both bulk phases and in the interphase. This means that a particular system will spontaneously evolve toward a state where both bulk solute concentrations can be different from what they were at the beginning. These equilibrium conditions will, therefore, be reached by a progressive transfer of solute atoms through the interface, by segregation and/or desegregation processes. Using the above equations and assumptions, the equilibrium bulk concentrations can be expressed as

$$X^{v}_{I1} = \frac{X^{v0}_{I1} + X^{v0}_{I2}}{1 + \exp\left(-\frac{\Delta G_{I1} - \Delta G_{I2}}{RT}\right)} \text{ and } X^{v}_{I2} = \frac{X^{v0}_{I1} + X^{v0}_{I2}}{1 + \exp\left(-\frac{\Delta G_{I2} - \Delta G_{I1}}{RT}\right)} \quad (13)$$

where X^{v0}_{I1} and X^{v0}_{I2} are the initial bulk concentrations.

The equilibrium state described by Eq. 10 corresponds to a stage where the fluxes between both bulk phases and the interphase, J_{I1} and J_{I2} are equal to zero. These fluxes are expressed in a manner similar to Eq. 3, as

$$J_{I1} = -\frac{D_{I1} C^{v}_{I1}(\varphi)}{\delta}\left(\frac{\Delta G_{I1}}{RT} + \ln\frac{\theta_I\left(1 - X^{v}_{I1}(\varphi)\right)}{X^{v}_{I1}(\varphi)(1 - \theta_I)}\right) \quad (14)$$

and

$$J_{I2} = -\frac{D_{I2} C^{v}_{I2}(\varphi)}{\delta}\left(\frac{\Delta G_{I2}}{RT} + \ln\frac{\theta_I\left(1 - X^{v}_{I2}(\varphi)\right)}{X^{v}_{I2}(\varphi)(1 - \theta_I)}\right) \quad (15)$$

Equations 14 and 15 are implemented in the FE software, along with two bulk diffusion models and an equation governing the evolution with time of the interfacial solute concentration, as in Eq. 4. The latter, nevertheless, takes into account the fluxes of solute exchanged with both bulk phases:

$$\frac{dC^{\varphi}_{I}}{dt} = -J_{I1} - J_{I2} \quad (16)$$

Finite element simulation and results

In practice, in the software there is a need to define two diffusion modes in the bulk (one for each phase) but only one "weak" mode in the interface to govern the evolution of interfacial concentration with time (since there is only

one segregating species). For the two diffusion modes, defined in a single geometry, the boundary conditions are the fluxes, expressed by Eqs. 14 and 15 and entered separately as "boundary expressions". For the interfacial "weak" mode, the boundary condition is expressed by Eq. 16.

No quantitative and usable data were found in the literature on interphase segregation (including free energies for segregation, experimental measurements of segregation kinetics, etc). To circumvent this lack of actual data, a "pseudo-virtual" illustrative example is chosen: the case of sulfur segregation at a silver–nickel interphase, for which hypothetical values have been considered for calculation. Another reason to use the Ni–Ag system is that silver and nickel are almost not miscible, and the interdiffusion between bulk elements can then be neglected. Arbitrarily, the free energies for segregation have been taken equal to the values for grain boundary segregation of sulfur in pure silver and pure nickel, respectively [14]: $\Delta G_{S,Ag} = -63$ kJ/mol and $\Delta G_{S,Ni} = -90$ kJ/mol. These values are probably not representative of real ones, but they are only used to illustrate physical phenomena in a qualitative manner and to assess the model on theoretical bases. Typical values for the diffusion coefficients of sulfur in silver and nickel are chosen, respectively, as follows: $D_{0,S,Ag} = 3.0 \times 10^{-5}$ m^2/s and $Q_{S,Ag} = 152$ kJ/mol [15]; $D_{0,S,Ni} = 1.4 \times 10^{-4}$ m^2/s and $Q_{S,Ni} = 219$ kJ/mol [1]. Calculations are performed at 900 °C with identical initial concentration of sulfur in Ag and Ni (100 at. ppm), no initial segregation in the interphase, and domains of 400 μm on each side of the interphase. Figure 6 presents the evolution of the coverage ratio with time. It first increases due to the high mobility of sulfur in silver (at 900 °C, $D_{S,Ag} = 5.1 \times 10^{-12}$ m^2/s and $D_{S,Ni} = 2.5 \times 10^{-14}$ m^2/s) and then reaches a plateau mainly due to the sole driving force for segregation of sulfur in silver. Then, when the effects of sulfur diffusion in nickel start to be significant, the coverage ratio again increases and tends toward a final equilibrium value of 0.107. Figure 7 presents the evolution of the bulk sulfur concentration with time, taken 10 μm away from the interface, in Ni and in Ag. It can be seen that, after a time long enough so that diffusion has significant effects in both metals, there is a progressive transfer of solute through the interphase, leading eventually to an adjustment of bulk concentrations to equilibrium values. The computed equilibrium concentrations are 188 at. ppm and 12 at. ppm, in silver and in nickel, respectively. This is in agreement with equilibrium conditions given by Eqs. 10–13. Figure 8 shows the solute concentration profiles in both phases after various times. Their evolutions confirm that a first "pseudo-equilibrium" is quickly reached, accompanied by a strong local solute depletion on the nickel side and by the establishment of a nearly flat profile on the silver side. It is followed by a

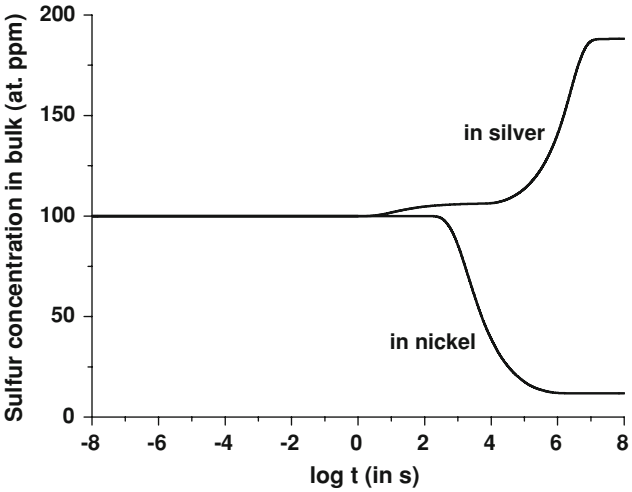

Fig. 7 Calculated evolutions of S concentration in bulk phases, 10 μm away from the interphase

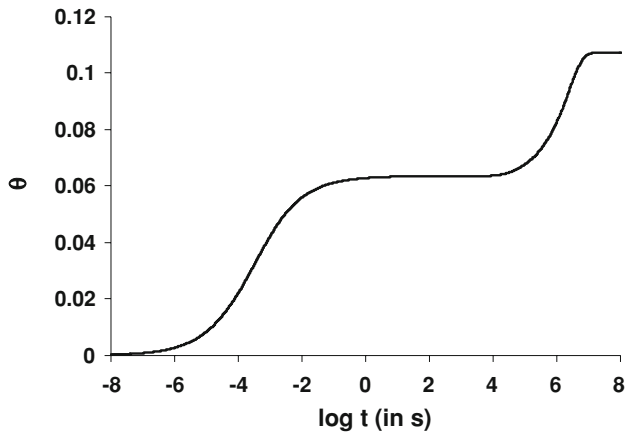

Fig. 6 Calculated segregation kinetics at an interphase between two metals

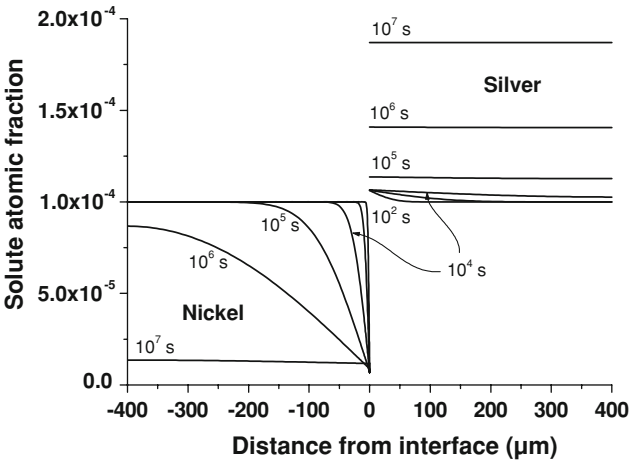

Fig. 8 Calculated S concentration profiles in bulk phases, after various times (10^2, 10^3, 10^4, 10^5, 10^6, and 10^7 s)

progressive transfer of solute across the interphase, the solute being rapidly "spread" on the silver side where diffusion is fast, whereas the profile on the nickel side progressively flattens to reach its equilibrium state.

Conclusions and perspectives

To sum up, interfacial segregation kinetics have been simulated by a FE method, by implementing, on the one hand, Fick's laws for bulk diffusion, and on the other hand, the Darken–Du Plessis equation at the interface. This article presents the development of a previously assessed model, which has been adapted to the case of complex interfacial phenomena:

(i) Segregation of a single dilute species with a solute–solute or solute–solvent interaction; the model is able to simulate physically meaningful kinetics, which tend toward published equilibrium data gained on the Ni–S system.
(ii) Simultaneous segregation of two species with a site competition in the interface; the model has been compared to published data in the case of the superficial cosegregation of P and S on an Invar alloy, which requires to add a P–S interaction parameter.
(iii) Segregation of a single species at an interface between two phases. A "virtual" Ni–Ag–S system has been simulated, with "arbitrarily" chosen values of the free energies of segregation.

In all the cases, the model is able to reproduce in a satisfactory manner the expected physical features of these segregation phenomena. Future study may include, for instance, the extension of the model to the case of a simultaneous bulk and surface/interface diffusion of solutes. This would require working on 2D or 3D models with complex meshes, instead of the 1D simulations, to be able to calculate not only diffusion in the bulk, but also diffusion inside the interface. Other prospects may concern the simulation of the simultaneous segregation of one (or several) species on two (or more) different interfaces, i.e., having different driving forces. Examples could include simultaneous surface and grain boundary segregation, or segregation to grain boundaries with different misorientations, hence exhibiting different free energies for segregation.

Acknowledgments The authors would like to acknowledge the support extended by Snecma Services (Safran Group) for this research through the funding for the Florent Founier Dit Chabert's PhD thesis, during which the original model was developed [6].

Appendix 1: Conversion of the raw AES measurements published in [11, 12] into surface coverage ratios

The Auger measurements presented in [11, 12] are expressed in ratios of Auger peak heights (see Fig. 4 of [12]) measured at 3 kV:

$$h_S = \frac{H_S}{1.3H_{Fe} + H_{Ni}} \text{ and } h_P = \frac{H_P}{1.3H_{Fe} + H_{Ni}} \quad (17)$$

where H_S, H_P, H_{Fe} and H_{Ni} the Auger peak heights of sulfur, phosphorus, iron, and nickel, respectively.

The atomic fraction of sulfur in the surface monolayer can be expressed as [16]

$$X_S^{\varphi} = \frac{1}{1 - \exp\left(-\frac{a}{\lambda \cos \alpha}\right)} \times \frac{\frac{H_S}{H_S^0}}{\frac{H_{Fe}}{H_{Fe}^0} + \frac{H_{Ni}}{H_{Ni}^0}} \quad (18)$$

where a is the thickness of the segregated layer, λ is the mean free path of the sulfur Auger electrons, α is the emission angle, H_S^0, H_{Fe}^0, and H_{Ni}^0 are the Auger sensitivity factors of sulfur, iron, and nickel respectively. The following values were chosen for the quantification of sulfur segregation: $a = 0.25$ nm [11], $\lambda = 0.596$ [11], $\alpha = 42.3°$ (CMA analyzer), $H_S^0 = 1.289$, $H_{Fe}^0 = 0.228$, and $H_{Ni}^0 = 0.255$ [17]. Eq. 18 becomes

$$X_S^{\varphi} = 0.46 \times \frac{H_S}{1.12H_{Fe} + H_{Ni}} \quad (19)$$

Assuming that $X_{S,max}^{\varphi} = 0.5$ [9], the sulfur coverage ratio can be expressed as

$$\theta_S = \frac{X_S^{\varphi}}{X_{S,max}^{\varphi}} = 0.92 \times \frac{H_S}{1.12H_{Fe} + H_{Ni}} \quad (20)$$

Equation 20 can reasonably be simplified as

$$\theta_S \approx h_S \quad (21)$$

Practically, the sulfur surface coverage ratio was then simply taken equal to the Auger peak height ratio, h_S, published in [11, 12] according to Eq. 21.

As far as phosphorus segregation is concerned, the following values were chosen: $a = 0.25$ nm [11], $\lambda = 0.5$ [16], $\alpha = 42.3°$ (CMA analyzer), $H_P^0 = 0.468$, $H_{Fe}^0 = 0.228$, and $H_{Ni}^0 = 0.255$ [17]. Furthermore, the value of $X_{P,max}^{\varphi}$ for phosphorus was assumed to be the same as $X_{S,max}^{\varphi}$ that for sulfur $\left(X_{P,max}^{\varphi} = X_{S,max}^{\varphi} = 0.5\right)$. The following quantification was obtained:

$$\theta_P = 2.22 \times \frac{H_P}{1.12H_{Fe} + H_{Ni}} \quad (22)$$

The phosphorus coverage ratio can then be reasonably calculated from the h_P values published in [11, 12] using the following equation:

$$\theta_P \approx 2.22 \times h_P \quad (23)$$

References

1. Cornen M (2006) Ségrégations intergranulaires d'impuretés dans le modèle Ni-S. PhD thesis, Université de Nantes, France
2. Hondros ED, Seah MP, Hofmann S, Lejček P (1996) In: Cahn RW, Haasen P (eds) Physical metallurgy, vol 2. North Holland, Amsterdam, pp 1201–1289
3. Ben Mostefa L, Saindrenan G, Solignac MP, Colin JP (1991) Acta Metall Mater 39:3111
4. Guttmann M, McLean D (1977) Interfacial segregation. ASM, Metals Park, USA
5. Du Plessis J, Van Wyk GN (1988) J Phys Chem Solids 49:1441
6. Fournier Dit Chabert F, Tancret F, Christien F, Le Gall R, Castagné JF (2007) J Mater Sci 42:9765. doi:10.1007/s10853-007-2001-3
7. Du Plessis J, Van Wyk GN (1989) J Phys Chem Solids 50:237
8. Darken LS (1949) Trans AIME 180:430
9. Larere A, Guttmann M, Dumoulin P, Roques-Carmes C (1982) Acta Metall 30:685
10. Saindrenan G, Le Gall R, Christien F (2002) Endommagement interfacial des métaux. Ellipses, Paris
11. Ben Mostefa Daho L (1990) Étude de la perte de ductilité à chaud des alliages Fe-Ni36 en relation avec les ségrégations interfaciales. PhD thesis, Université de Nantes, France
12. Ben Mostepha L, Roptin D, Saindrenan G (1990) Mater Sci Technol 6:885
13. Menyhard M (1991) Surf Sci Lett 258:L683
14. Aufray B, Cabane-Brouty F, Cabane J (1979) Acta Metall 47: 1849
15. Ladet J, Aufray B, Moya F (1978) Metal Sci 12:195
16. Seah MP (1990) Practical surface analysis, vol 1—Auger and X-ray photoelectron spectroscopy. Wiley, New York, p 201
17. Davis LE, McDonald NC, Palmberg PW, Riach GE, Weber RE (1978) Handbook of Auger electron spectroscopy, 2nd edn. Physical Electronics Division, Perkin-Elmer Corporation, Eden Prairie